

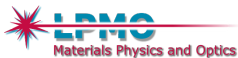
# Optical properties of plasmonic nanocomposites at the (sub)micron scale

## WORKSHOP – Photonic composite elastomers

**Michel Voué**

University of Mons  
Physics of Materials and Optics  
Research Institute for Materials Science and Engineering  
Mons - Belgium

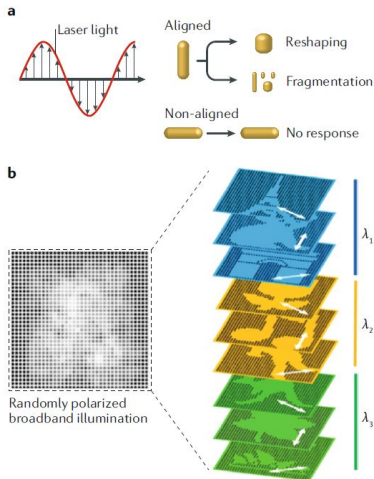
August 27, 2024





# Plasmonic nanocomposites (PNCs)

- ▶ Plasmonic nanoparticles have been developed for multiple purposes : detection of chemicals and biological molecule, light-harvesting enhancement in solar cell ...
- ▶ PNCs : Hybrid materials synthesized by adding plasmonic nanoparticles to a polymer matrix
- ▶ Robustness, responsiveness and flexibility of the system are enhanced
- ▶ Intrinsic properties of the nanoparticles preserved
- ▶ Applications in optical data storage, sensing and imaging and photothermal gels for in vivo therapy



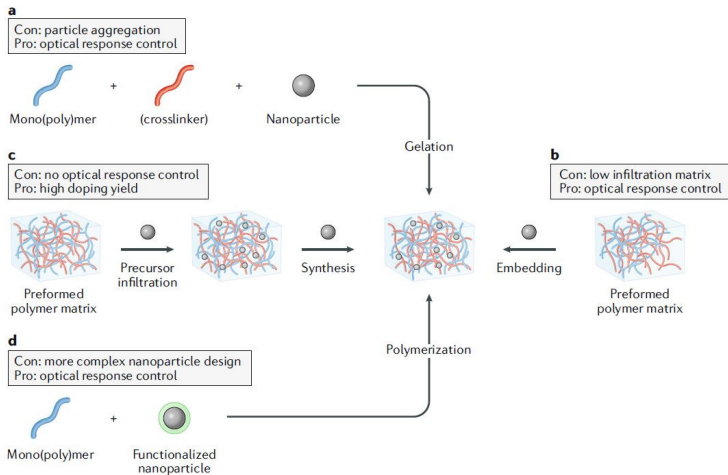
Pastoriza-Santos *et al*, Nature Reviews Materials (2018)  
DOI : 10.1038/ s41578-018-0050-7

# PNCs when PNCs were not named "PNC"...



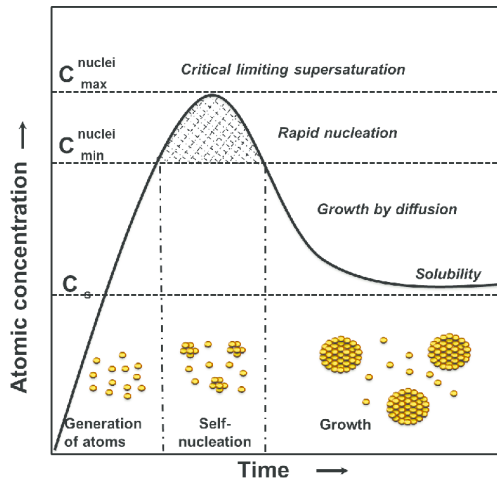
(A) - (B) Pictures of the Lycurgus cup (from the British Museum Images, London). (A) Lit from the outside and (B) illuminated from the inside. (C) Stained glass "*Les joueurs d'échecs*" from the Cluny Museum, Paris.

# Synthesis scheme



Pastoriza-Santos *et al*, Nature Reviews Materials (2018)  
DOI : 10.1038/ s41578-018-0050-7

# Lamer's diagram for colloidal solutions (1950)



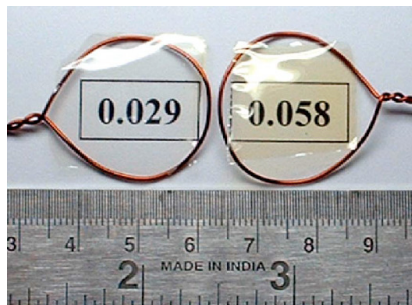
## Formation process of monodisperse particles.

$C_0$  : equilibrium concentration of solute with the bulk solid,  $C_{nuclei\ min}^{nuclei}$  : critical concentration as the minimum concentration for nucleation, respectively. (I) prenucleation : generation of atoms, (II) self-nucleation, and (III) growth stages, respectively (Lamer and Dinegar, 1950).

Valid for solutions → also valid for thin films ?

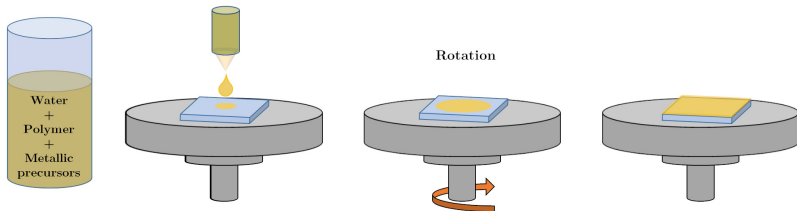
# First main study of the PVA/AgNPs system

(Free standing films)



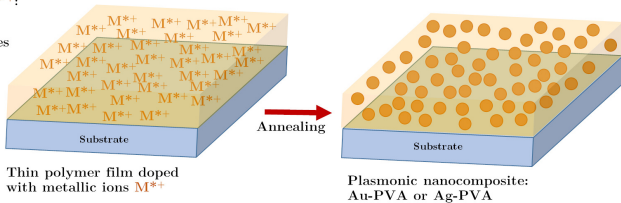
Photographs of free-standing films of AgNPs in PVA matrix ; transparency of the films is demonstrated by placing them on wire frames above a paper on which the corresponding value of the Ag/PVA mass ratio is printed (Porel, 2007).

# Experimental protocol in more details ...



Metallic precursors  $M^{*+}$ :

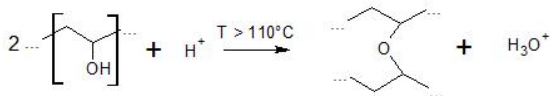
- $\text{HAuCl}_4 \cdot 3\text{H}_2\text{O}$   
for gold nanoparticles
- $\text{AgNO}_3$  for silver nanoparticles





# In situ reduction scheme of $\text{Ag}^+$

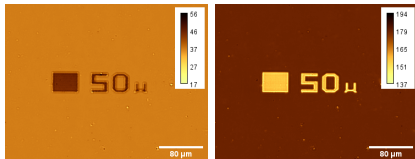
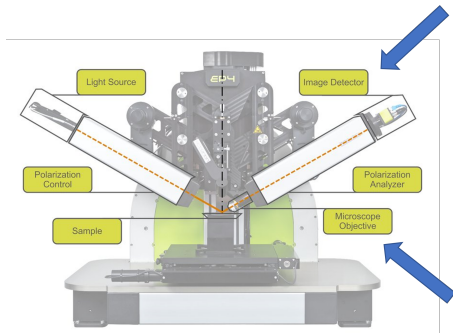
- ▶ Temperature for reduction :  $T > 90^\circ\text{C}$
- ▶ Higher than the glass transition temperature of the polymer matrix ( $T_g = 85^\circ\text{C}$ )
- ▶ For  $T > 110^\circ\text{C}$  : crosslinking of the polymer matrix and less solubility to  $\text{H}_2\text{O}$



(Top) Reduction scheme for the silver cations. (Bottom) Cross-linking of the PVA chains at high temperature (redrawn from Nicolais, 2014)

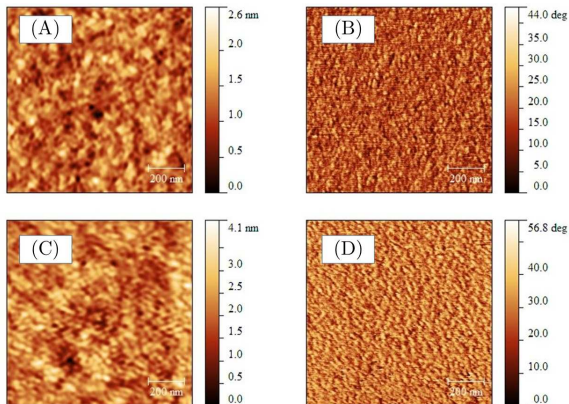
# Imaging Ellipsometry (IE)

- ▶ combines **optical microscopy** and **ellipsometry** for spatially resolved layer-thickness and refractive index measurements of **micro-structured thin-films and substrates**.
- ▶ produces after optical modelling **images (maps)** of the measured quantities (thickness, refractive index, composition) at a spatial resolution of 1  $\mu\text{m}/\text{pixel}$



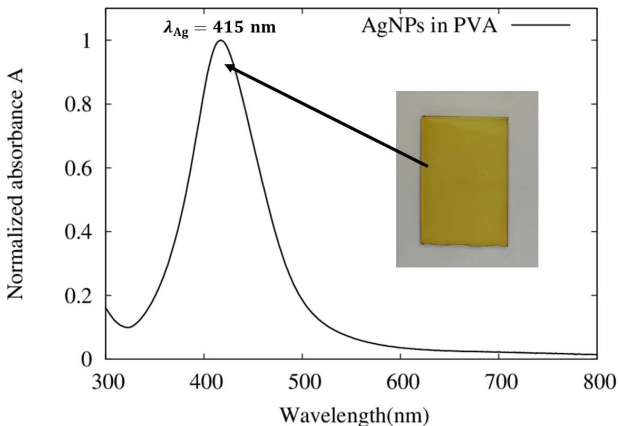
$\Psi$  and  $\Delta$  maps of a **100nm-thick  $\text{SiO}_2$  pattern** on native oxide (Image at 658nm)

# Topography of the PVA films by AFM



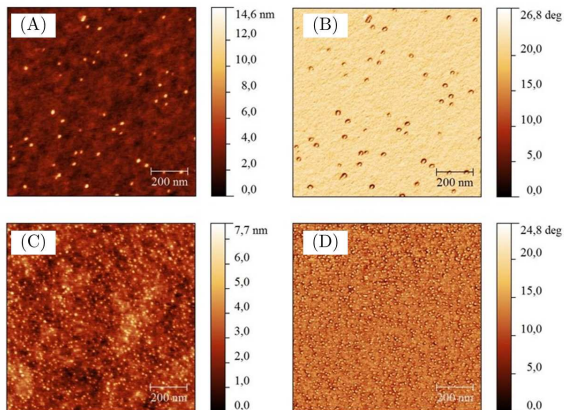
AFM topographic (left) and phase (right) images of the PVA control films. (A,B) 30 nm-thick films (C,D) 300 nm-thick films. Image size :  $1 \mu\text{m} \times 1 \mu\text{m}$  ( $256 \times 256$  pixels).

# UV-Vis spectra of AgPVA PNCs



Absorption spectrum of a glass coated with a thick film of AgNPs embedded in a PVA matrix at high doping level ( $[Ag]/[PVA] = 25\% \text{ w} : \text{w}$ ). The inset picture is the analyzed sample.

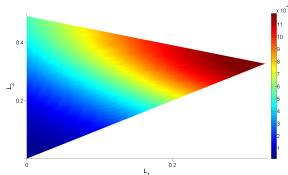
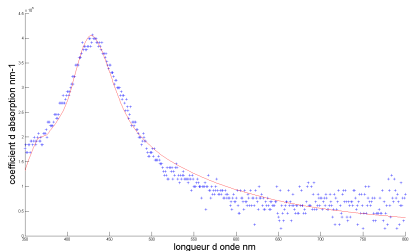
# Topography of the Ag-PVA films



Topography (left) and phase (right) AFM images of Ag-PVA film doped with 25%  $\text{AgNO}_3$  (w : w). (A, B) :  $\simeq 30$  nm-thick film ; (C, D) :  $\simeq 300$  nm-thick film. Image size :  $1 \mu\text{m} \times 1 \mu\text{m}$  ( $256 \times 256$  pixels).

# Depolarisation factor analysis : NPs shape analysis

(Y. Battie, A. En Naciri, UDL)



Ag-PVA film (8/2.5) – film thickness  $\simeq 30$  nm : (Left) Modelling of the extinction spectra of a - (Right) Distribution of the depolarisation factors

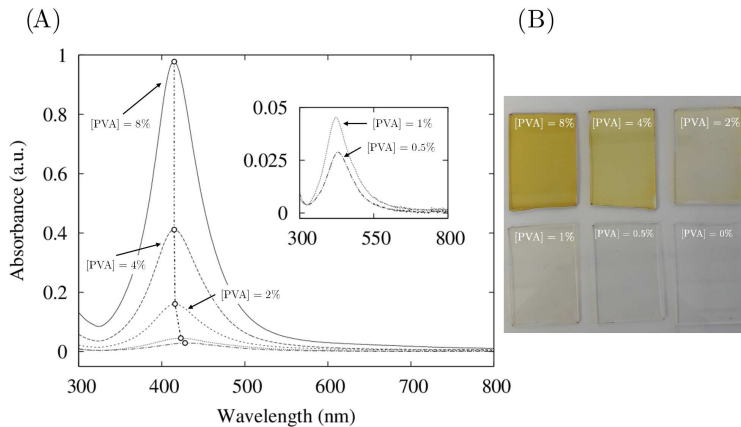
Distribution centred around (1/3, 1/3, 1/3) : **Spherical NPs**

# Film thickness effect at constant metal/polymer mass ratio

Samples ID	Polymer conc. (%)	Thickness (nm)	RMSE
[PVA] = 8%	8	$374.9 \pm 1.4$	1.683
[PVA] = 4%	4	$121.1 \pm 0.1$	0.709
[PVA] = 2%	2	$54.5 \pm 0.3$	0.271
[PVA] = 1%	1	$28.9 \pm 0.1$	0.205
[PVA] = 0.5%	0.5	$15.8 \pm 0.1$	0.093

Measured thicknesses of the silver nanocomposite by the EP3-SE using Cauchy model. The model is applied on the ellipsometric data far from the resonance, i.e. for incident wavelength larger than 545 nm.

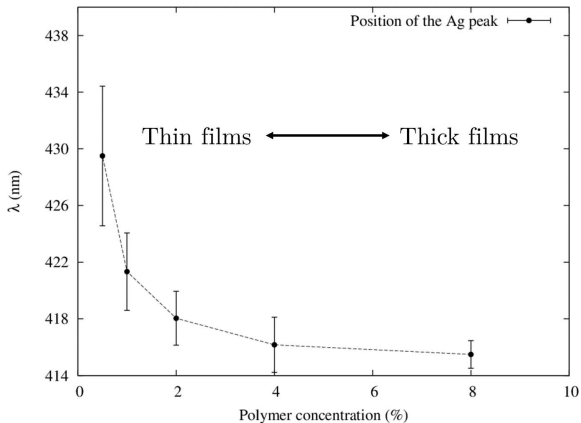
# Film thickness (unexpected) effect



(A) Absorption spectra. Inset : Details for the thinner films. (B) Picture of the analysed samples.



# Red-shift of the resonance peak



Position of the resonance peak as a function of the polymer concentration.

# Factors inducing thickness-controlled optical properties

- ▶ Diffusion via the molecular mass of the polymer (entanglement of the polymer chains)
- ▶ Thickness of the film
- ▶ Substrates effects

Thick layers (240 nm)		Thin layers (14 nm)	
PVA	$\lambda_{spr}$ (nm)	PVA	$\lambda_{spr}$ (nm)
13-23 kDa	417	13-23 kDa	434
13-23 kDa	417	13-23 kDa	432
31-50 kDa	417	85-124 kDa	433
31-50 kDa	418	85-124 kDa	435

# Modelling of the optical properties $\epsilon = (n - j k)^2$

**PVA layer** : A one-layer Cauchy model is chosen to represent the optical properties of the PVA films in the transparent range

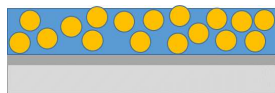
$$n_{\text{PVA}}(\lambda) = A_{\text{PVA}} + \frac{B_{\text{PVA}}}{\lambda^2} \quad \text{and} \quad k_{\text{PVA}}(\lambda) = 0$$

**Ag-PVA layer** : A Lorentzian oscillator is added to that model to account for the localized absorption of the plasmon resonance in visible range.

$$\epsilon(\lambda) = \epsilon_r(\lambda) + i\epsilon_i(\lambda)$$
$$\epsilon_r(\lambda) = \epsilon_\infty + \frac{A\lambda^2 (\lambda^2 - \Lambda_0^2)}{(\lambda^2 - \Lambda_0^2)^2 + \Gamma_0^2 \lambda^2} \quad \epsilon_i(\lambda) = \frac{A\lambda^3 \Gamma_0}{(\lambda^2 - \Lambda_0^2)^2 + \Gamma_0^2 \lambda^2}$$

( $\lambda$  : wavelength,  $\Lambda_0$  : resonance wavelength of the oscillator,  $A$  : oscillator strength,  $\Gamma_0$  : full-width at half maximum (FWHM),  $\epsilon_\infty$  : contributions of the resonances at wavelengths  $\gg$  than the measurable wavelength range.

# Schematic representation of the optical model of Ag-PVA



(A)

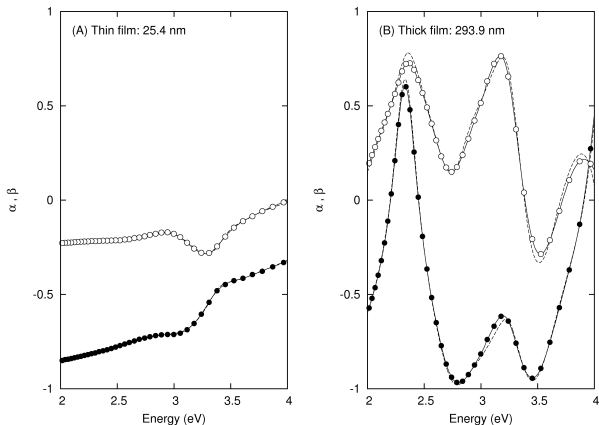


(B)



Schematic representation of the optical model used to interpret SE data : (A) AgNPs in PVA layer on Si and (B) a Cauchy model and Lorentzian oscillator used to describe the optical properties of AgNPs in PVA matrix. (Not to scale)

# Ellipsometric spectra of Ag-doped PVA films



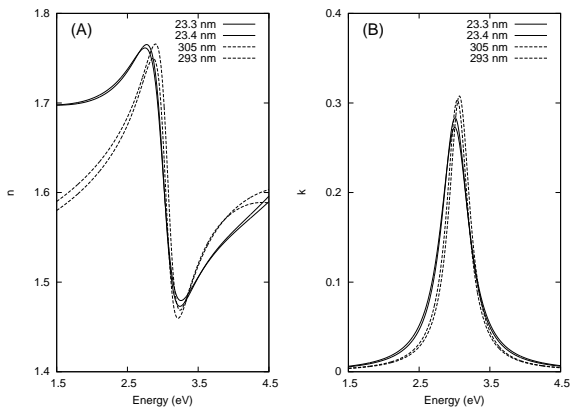
A, 'tH' thin films (thickness : 25.4 nm) ; B, 'TH' thick film (thickness : 293.9 nm).  
Experimental data :  $\alpha = \cos(2\Psi)$  (filled circles) and  $\beta = \sin(2\Psi) \cos(\Delta)$  (open circles).  
Dashed lines : optimized results from the optical model. ([Ag]/[PVA] ratio : 25% w :w)

# Parameters of the plasmon absorption peak

Sample	d (nm)	A	$\Lambda_0$ (nm)	$\Gamma_0$ (nm)
Thin	$23.4 \pm 0.2$	$0.145 \pm 0.006$	$414.2 \pm 0.7$	$67.6 \pm 2.9$
	$25.4 \pm 0.3$	$0.133 \pm 0.005$	$415.6 \pm 0.6$	$69.0 \pm 2.6$
Thick	$305.9 \pm 1.7$	$0.117 \pm 0.002$	$405.4 \pm 0.7$	$47.3 \pm 1.6$
	$293.4 \pm 1.7$	$0.118 \pm 0.002$	$409.5 \pm 0.6$	$49.2 \pm 1.5$

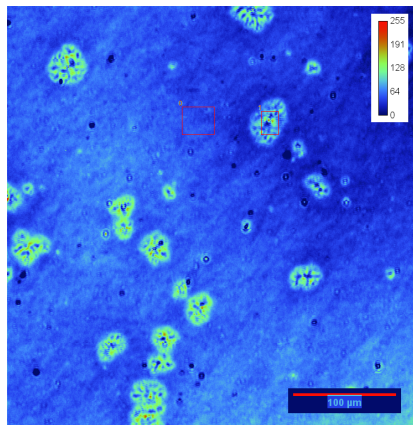
Typical parameters of the plasmon absorption peak

# Optical properties of thin and thick Ag-doped PVA films



Optical properties of thin (plain lines) and thick (dashed lines) silver NPs-doped PVA films ([Ag]/[PVA] ratio : 25% w :w) : A, refractive index  $n$ ; B, extinction coefficient  $k$ .

# Ellipsometric enhanced contrast (EEC) images at high silver concentration

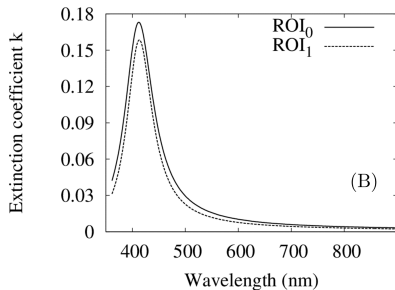
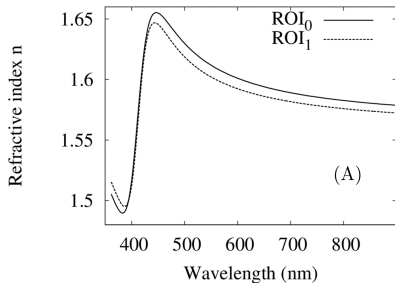


Ellipsometric enhanced contrast (grey levels, in false color) image of the Ag–PVA film at the end of the annealing (Scalebar :  $100\ \mu\text{m}$ , wavelength :  $545\ \text{nm}$ , AOI :  $42^\circ$ ). Red rectangles indicates the regions of interest "0" and "1" used for spectroscopic characterization.

Visualize – Identify – Measure



# Local optical properties



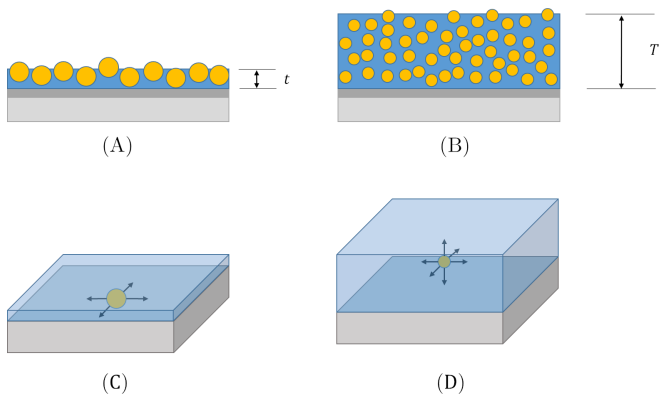
Optical properties of 445.7 nm-thick silver nanocomposite film ([Ag] : [PVA] ratio : 25% w : w) : A, refractive index  $n$ ; B, extinction coefficient  $k$ .

# SIE local fits for Ag-PVA films

**Table 1** – Best-fit results of the ellipsometric data obtained with the SIE on AgNPs embedded in PVA matrix within the Lorentzian term in order to take into account the absorption peak.

ROI	Thickness (nm)	Amplitude (eV <sup>2</sup> )	Frequency (eV)	Damping (eV)	RMSE
0	445.7 ± 3.0	0.786 ± 0.021	3.000 ± 0.014	0.480 ± 0.021	3.179
1	445.2 ± 3.3	0.608 ± 0.021	2.979 ± 0.012	0.378 ± 0.027	3.405

# Scheme of the NPs growth (2D vs 3D growth)



# Modelling of the NPs growth : diffusion/aggregation

- ▶ Langevin dynamics with coarse grain approximation (no explicit description of the polymers)

$$m\ddot{x}(t) = -\nabla U[x(t)] - \gamma m\dot{x}(t) + R(t)$$

where  $\gamma$  is a damping constant,  $U$  the particle interaction potential and  $R(t)$  a random-force vector whose statistical properties are given by

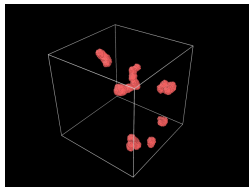
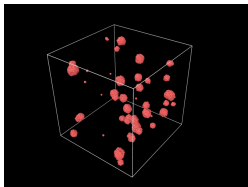
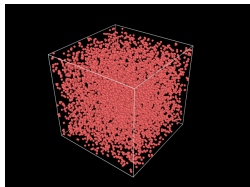
$$\langle R(t) \rangle = 0 \quad \text{and} \quad \langle R(t)R^T(t') \rangle = 2m\gamma k_B T \delta(t - t')$$

- ▶ LAMMPS (simulation) and OVITO (visualization and analysis)
- ▶ Tracers diffusion in a viscous medium with possibility of aggregation (6-12 LJ potential between the tracers)
- ▶ Several periodic boundary conditions (bulk, thick and (very) thin films)
- ▶ Constant number of tracers
- ▶ Constant volume of the simulation cell
  
- ▶ Interaction parameters between the tracers
- ▶ Friction between the tracers and the effective medium  $\longrightarrow$  effect of the viscosity

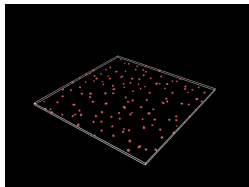
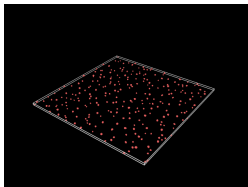
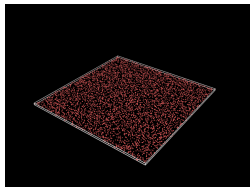
# Snapshots

(7200 tracers, timesteps : 0,  $125.5 \times 10^3$ ,  $500 \times 10^3$ )

## Thick films (100 x 100 x 100)



## Thin films (400 x 400 x 6)



# Geometrical features of the clusters

- **Gyration tensor** : tensor describing the second moments of position of a collection of particles

$$G_{mn} = \frac{1}{N} \sum_{i=1}^N \sum_{j=1}^N (r_m^i - r_m^j)(r_n^i - r_n^j),$$

where  $N$  is the number of particles,  $r_m^i$  is the  $m^{\text{th}}$  cartesian coordinate of the position vector  $r^i$  of the  $i^{\text{th}}$  particle.

- **Gyration radius** : After diagonalization of the gyration tensor ( $\lambda_i, i = 1, \dots, 3$ )

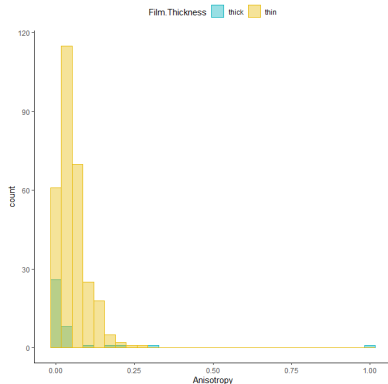
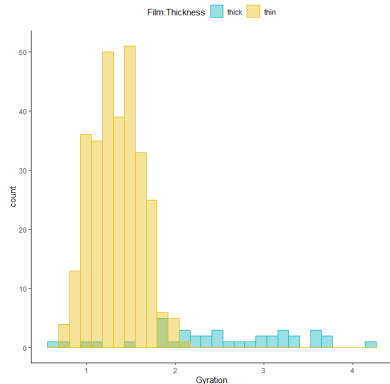
$$R_g^2 = \frac{1}{N}(\lambda_x^2 + \lambda_y^2 + \lambda_z^2)$$

- **Asphericity** ( $b$ ), **Acylindricity** ( $c$ ), **Anisotropy factor** ( $k$ )

$$b = \lambda_z - \frac{(\lambda_y + \lambda_x)}{2} \quad c = \lambda_y - \lambda_x,$$

$$k = \frac{3}{2} \frac{(\lambda_x^2 + \lambda_y^2 + \lambda_z^2)}{(\lambda_x + \lambda_y + \lambda_z)^2} - \frac{1}{2}.$$

# Cluster analysis : some statistics



- ▶ Thin films : more clusters, smaller  $R_g$  and increased anisotropy
- ▶ Thick films : less clusters, larger  $R_g$  and less anisotropy (more spherical)

# Conclusions, prospects and open questions

- ▶ Influence of the film thickness on the intrinsic optical properties
  - ▶ Red shift of the resonance band for thin films at constant metal/polymer mass ratio
  - ▶ Spherical nanoparticles in thick films
  - ▶ No influence of the polymer mass (pure diffusion) at constant thickness
  - ▶ Diffusion/aggregation model via molecular dynamics or Monte-Carlo methods : divergence from the spherical shape in very thin films in agreement with experimental observations
- 
- ▶ "Real" distribution of the NPs in thin films by AFM, SEM or TEM
  - ▶ Extension to NPs with other particle shapes
  - ▶ Multilayered PNCs as model for hyperbolic metamaterials



# Acknowledgements

- ▶ Dr. Corentin Guyot (Formerly : LPMO, now : B-Sens Technology, Mons)
- ▶ Pr. Philippe Leclère (UMONS)
- ▶ Dr. Peter Thiesen & Dr. Mathias Duwe (Accurion GmbH, Gottingen)
- ▶ Clémence Mimoso, Tim Willame (MA students)
- ▶ FRS-FNRS
- ▶ UMONS – Research Institute for Materials Science and Engineering



**Thank you for your attention**